Macromolecular Bioscience
www.mbs-journal.de

A Reusable Column Method Using Glycopolymer-Functionalized Resins for Capture–Detection of Proteins and *Escherichia coli*

*Juby K. Ajish, Hephziba Maria Abraham, Mahesh Subramanian, and K. S. Ajish Kumar**

The use of glycopolymer-functionalized resins (Resin–Glc), as a solid support, in column mode for bacterial/protein capture and quantification is explored. The Resin–Glc is synthesized from commercially available chloromethylated polystyrene resin and glycopolymer, and is characterized by fourier transform infrared spectroscopy, thermogravimetry, and elemental analysis. The percentage of glycopolymer functionalized on Resin–Glc is accounted to be 5 wt%. The ability of Resin–Glc to selectively capture lectin, Concanavalin A, over Peanut Agglutinin, reversibly, is demonstrated for six cycles of experiments. The bacterial sequestration study using SYBR (Synergy Brands, Inc.) Green I tagged *Escherichia coli*/*Staphylococcus aureus* reveals the ability of Resin–Glc to selectively capture *E. coli* over *S. aureus*. The quantification of captured cells in the column is carried out by enzymatic colorimetric assay using methylumbelliferyl glucuronide as the substrate. The *E. coli* capture studies reveal a consistent capture efficiency of 10^5 CFU (Colony Forming Units) g^{-1} over six cycles. Studies with spiked tap water samples show satisfactory results for *E. coli* cell densities ranging from 10^2 to 10^7 CFU mL^{-1}. The method portrayed can serve as a basis for the development of a reusable solid support in capture and detection of proteins and bacteria.

1. Introduction

With drastic developments going on in the field of human health and hygiene, pathogenic bacterial/viral infection and microbial contamination still remain a serious problem. This is because the time-consuming conventional techniques like bacterial culturing and plate counting are still being followed in clinical diagnosis.[1,2] These methods often require a few days to obtain the results, in which case, the total number of the cultured bacteria can be underestimated, as some specific bacteria can enter a viable but nonculturable state in environment.[3,4] In order to counter this, real-time polymerase chain reaction (PCR)-based assays are commonly used in laboratory for rapid bacterial detection. But a major limitation of PCR, particularly for low concentration of bacterial cells, is the time required for enrichment, which is often 6–48 h.[5–10] In addition, the equipment cost and requirement of highly trained personnel limit the usage of PCR-based assays. An alternative is enzyme-linked immunosorbent assays (ELISA), which are rapid but laborious, with a detection limit in the range as high as 10^4–10^6 CFU mL^{-1}.[11] However, these rapid detection procedures usually require extensive sample preparation steps with the concentration of the sample as the major limiting factor.[12–17]

To overcome the above shortcomings, various biosensors have been developed, particularly, to reduce assay time and to improve the sensitivity. Many sensor-based methods, like label-free immune-based biosensors, have a lower detection limit (2 CFU mL^{-1}), but the requirement of assay volume limited to micro liters to milliliter range makes detection at very low concentration cumbersome.[18] Often monitoring of contamination in food industries and environmental screening involves large volume of the initial water sample (100–1000 mL).[19] In a contaminated water sample with a bacterial concentration of 100 CFU/100 mL, the assay volume for bacterial detection should be as minimum as 1 mL, so that at least one cell is included in the tested assay.[20] Therefore, the single cell detection biosensors cannot be used for practical rapid detection in terms of the total assay volume. Hence, there is an urgent requirement to have an access to a rapid, simple, and effective system for selective capture as well as concentration of target bacteria and then release them for the rapid assessment or downstream analysis. In recent decades, surface modification techniques based on "capture-and-release" strategy have been reported for the isolation or detection of cancer cells or tissue cells.[21,22] Solid supports like magnetic and gold nanoparticles (AuNPs) functionalized with mannose conjugated

Dr. J. K. Ajish
Radiation and Photochemistry Division
Bhabha Atomic Research Centre
Trombay, Mumbai 400085, India
H. M. Abraham
Department of Polymer Science and Rubber Technology
Cochin University of Science and Technology
Kochi 682020, India
Dr. M. Subramanian, Dr. K. S. Kumar
Bio-Organic Division
Bhabha Atomic Research Centre
Trombay, Mumbai 400085, India
E-mail: ajish@barc.gov.in
The ORCID identification number(s) for the author(s) of this article can be found under https://doi.org/10.1002/mabi.202000342.

DOI: 10.1002/mabi.202000342

β-cyclodextrin derivatives, carbohydrate-functionalized graphene derivatives etc. have been used for capture and release of bacteria by host–guest interactions.[23–25]

Major approaches for separating food-borne bacteria and their concentration include those based on biological interactions such as immunomagnetic separation (IMS),[26–31] antigen–antibody interaction, ligands such as aptamers,[32,33] bacteriophages,[34] and other binding molecules.[33] Magnetic-bead-based separation for bacteria has several advantages, like specific removal of target from food particles,[34–36] no dilution of sample or carrier during washing, and possible automation and scale-up separation.[37–39] In spite of these advantages, the longevity of the biological material attached to magnetic particles, interferences in food matrices, the strength of the magnetic field, sufficient mixing to maximize the interactions, etc. are some of the obstacles associated with this method.[40] This is where immobilized molecules on solid surfaces find application for direct capture to the detector surface for analysis and removal of unbound substances in the samples by washings.[41–44] The immobilization of bacteria-specific ligand is also an important factor for effective bacterial capture.[45,46] Antibody- and aptamer-based ligands are highly selective and have strong binding affinity for specific bacterial strains.[47,48] However, their application is limited by the high cost and low stability. Alternatively, carbohydrate-based ligands have received considerable attention because they are cost-effective, less prone to denaturation, and have broader interaction specificity.[49–51] Different surface modification techniques such as chemical linkers self-assembled monolayers (SAM), antibody-oriented immobilization, and biomolecule labels are being used to immobilize various ligands.[52,53] Reusability of the surface is an important criteria to be fulfilled to make the method cost effective.[54]

Studies on bacteriophilic resins started in the 1950s, mostly for targeting viruses, which were later extrapolated to bacteria, essentially *Escherichia coli*, *Salmonella*, *Shigella dysenteria*, and *Staphylococcus aureus* strains.[55] Limited studies are directed toward water bacterial disinfection by flocculation[56] or clustering of bacteria, adhesion of bacteria on insoluble beads[57] or clothes.[58] Stenzel and co-workers have reported crosslinked glucose-based latex glycol particles, which can bind to lectins as well as bacteria.[59]

The incorporation of carbohydrate moieties into polymeric materials is highly significant because of their molecular recognition properties.[60] Therefore, stationary phases or solid supports immobilized with sugar units find application in the study of lectin, saccharide-specific recognition processes, protein separation, and purification procedures.[61] In this direction, Haddleton and co-workers successfully demonstrated loading of carbohydrate on to Wang resin beads using copper-catalyzed Huisgen cycloaddition.[62] Glycopolymers can also be grafted onto microspheres employing thiol–ene reactions, Michael addition reactions, etc.[63] Fluorostyrene-based microspheres bearing carbohydrate moieties have also been synthesized as the support for protein separation.[64] Recently, we have reported the use of synthetic glycoacrylamides as well as glycoacrylamide-stabilized AuNPs for lectin/bacterial detection.[65,66] By virtue of its self-assembly behavior, the much needed condition of multivalency effect is met by these small glycounits for the detection of carbohydrate-interacting systems. In the present study, we make use of the "glycocluster effect" present in the glycopolymer derived from glycoacrylamide (**1**) (**Figure 1**), synthesized in our laboratory,[67] for making reusable glycopolymer-functionalized resins for efficient capture and detection of lectin/bacteria. The system that we foresee is unique not only in terms of its robustness and economical nature, with the possibility to easy scale up, but also in the fact that we can recover these resins without loss of its activity, in an effortless manner.

Using this capture–detection strategy concentration of the glyco-interacting species present in the samples will no longer be a limitation. We envisaged that the amino-functionalized resin generated from commercial chloromethylated polystyrene divinylbenzene resin (Resin–Cl) could be coupled to the glycopolymer (glycoacrylamide–acrylic acid (Glc–AA)) which would serve as the template for bacterial/protein capture (Figure 1). Using bacterial protein extraction reagent (B-PER), the glucouronidase enzyme liberated from the captured bacteria is collected and quantified using 4-methylumbelliferyl-β-D-glucoronide (4-MUG)-based assay. To the best of our knowledge, this is the first report on a reusable column method using resin functionalized with glycopolymer for capture and quantification of Concanavalin A (Con A)/*E. coli*.

2. Experimental Section

2.1. Materials

Lyophilized powders of Con A from *Canavalia ensiformis*, peanut Agglutinin (PNA) from *Arachis hypogaea*, fluorescein isothiocyanate (FITC) conjugates of both Con A (FITC–Con A) and PNA (FITC–PNA), sodium azide, *N*-hydroxy succinimide (NHS), 1-ethyl-3-(3-dimethylaminopropyl)carbodiimide (EDC), triphenylphosphine, β-glucuronidase (β-GUS), 4-MUG, and SYBR Green I were purchased from Sigma–Aldrich and were used directly. B-PER was purchased from ThermoFischer Scientific. Dimethyl formamide (DMF), methanol, dichloromethane, and acrylic acid were purchased from SD-fine. Chloromethylated styrene divinylbenzene resins were purchased from Thermax India Pvt. Ltd. 0.01 M phosphate-buffered saline (PBS) at pH 7.4 was freshly prepared by diluting 10× concentrated PBS purchased from Sigma into distilled water to 1×10^{-3} M $CaCl_2$ and 1×10^{-3} M $MnCl_2$. Dulbecco's modified eagle's medium (DMEM), penicillin, and streptomycin were purchased from Hi-Media, Mumbai, India. Fetal bovine serum (FBS) was procured from Invitrogen BioServices India Pvt. Ltd. Water with a conductivity of 0.6 μS cm^{-1} or lower, obtained from Millipore Milli-Q system, was used for the preparation of aqueous solutions. Glasswares were cleaned, using chromic acid, rinsed with distilled water, and then with Millipore Milli-Q water before drying in an oven at 110 °C. D-glucose-based acrylamide (**1**) was synthesized as per the previous report.[67] Wild-type *E. coli* K12 strain BW25113 was grown overnight in lysogeny broth (LB) at 37 °C till the value of A_{600} was 1.0. Cell mixture (1 mL) was centrifuged (10 000 rpm, 20 min, 4 °C) and washed twice with PBS buffer. These cells were resuspended in PBS buffer (1.0 mL) containing $CaCl_2$ (0.1×10^{-3} M) and $MnCl_2$ (0.1×10^{-3} M) and were serially diluted to the required concentrations. The same procedure was followed with *S. aureus* strain, which does not possess mannose/glucose binding protein, FimH.

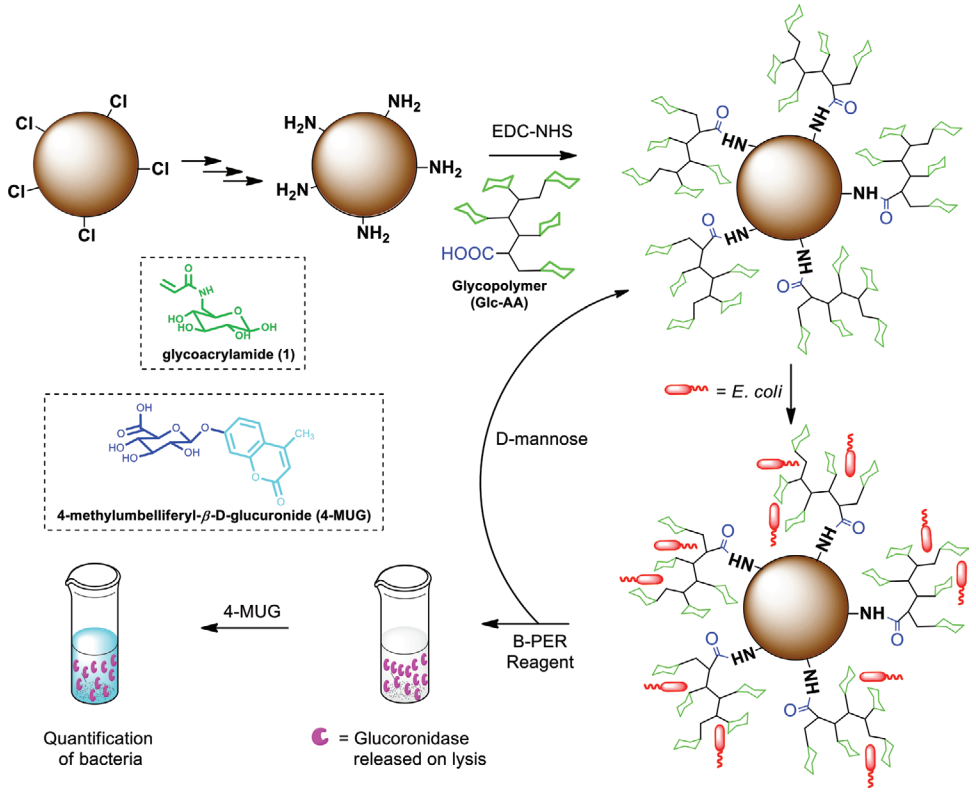

Figure 1. Schematic representation of synthesis of glycopolymer-functionalized resin (Resin–Glc) for capture and quantification of *E. coli*/Con A.

2.2. Methods

2.2.1. Fourier Transform Infrared Spectroscopy

The IR spectra were recorded using a diamond single reflectance ATR in Shimadzu IR Affinity-1 spectrometer. The samples were analyzed over the range of 400–4000 cm^{-1}, operating at 4 cm^{-1} resolution.

2.2.2. Thermogravimetric Analysis

Thermogravimetric analysis (TGA) was performed, using a Mettler-Toledo TG/DSC star^e system. The samples were analyzed in the temperature range of 25–600 °C at a heating rate of 10 °C min^{-1} and a nitrogen flow rate of 50 mL min^{-1}.

2.2.3. Photography

The optical photographs were taken by a digital camera (Sony cybershot). For viewing UV-active samples, a conventional hand-held UV lamp (λ = 365 nm, Cole-Parmer Ultraviolet lamps) was used for illumination, and was photographed.

2.2.4. Synthesis of Glycopolymer: Glc–AA

Glycoacrylamide (**1**) was copolymerized with acrylic acid (**2**), using ammonium persulfate (APS) as initiator at an initiation temperature of 60 °C for 12 h (**Scheme 1**). Briefly, a two-necked round bottom flask, under argon atmosphere, was charged with glycoacrylamide (0.15 g, 0.64 mmol) dissolved in deionized water (50 mL); to it, acrylic acid (4.40 µL, 0.064 mmol

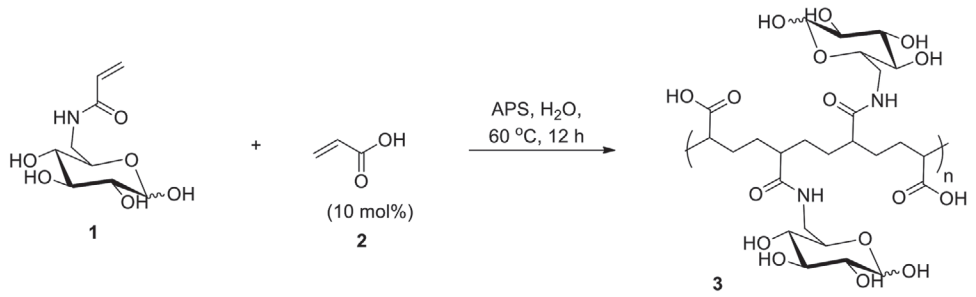

Scheme 1. Synthesis of glycoacrylamide–acrylic acid (Glc–AA) copolymer.

(10 mol% of glycoacrylamide)) was added and stirred for 1 min. The resultant homogeneous solution was heated to 60 °C in oil bath; APS (8.30 mg, 0.04 mmol) was added; and the reaction was stirred for 12 h. The reaction was cooled to room temperature and was purified using dialysis membrane (Spectrum Labs Spectra/Por 1000 D MWCO Standard RC Pre-wetted Dialysis Kit). The leftover solution in the dialysis membrane was lyophilized to afford glycopolymer (Glc–AA) (**3**) as a white amorphous fluffy solid (0.11 g). ^{1}H NMR spectra were recorded on 500 MHz Varian instrument using D_2O as the solvent (Figures S1 and S2, Supporting Information). The Fourier Transform Infrared (FTIR) spectrum analysis (Figure S3, Supporting Information) of (**3**) revealed the presence of characteristic bands of carboxylate functionality at 1727 and 1249 cm^{-1} while bands at 1651 and 1622 cm^{-1} were assigned to amide I and amide II bands due to polyamide units and a combination band of OCH and COH deformations present at 1552 and 1421 cm^{-1} confirms the structural integrity of glycopolymer (**3**).

2.2.5. Synthesis of Glycopolymer (Glc–AA)-Functionalized Resins

Chloromethylated styrene divinylbenzene resins with 5.20 mmol g^{-1} substitution of chlorine were converted to their azide derivatives by reacting with sodium azide in DMF at 90 °C (**Scheme 2**).

The resultant azide-substituted resins were subjected to the Staudinger reaction to furnish corresponding amine-functionalized resins as confirmed by FTIR spectroscopy. The amine-functionalized resins were then coupled with Glc–AA (**3**) using the EDC–NHS method in DMF–water to afford glycopolymer-functionalized resins, Resin–Glc (**4**). The free carboxylic acid groups in (**4**) were converted to amide, Resin–Glc–MeNH$_2$ (**5**) (FTIR, Figure S4, Supporting Information), by coupling with methyl amine using EDC–NHS as mentioned in Scheme 2. Resin–Glc (**4**) and (**5**) were used in the *E. coli* capture studies. Synthetic procedures for the functional modification of resin are described in Schemes S1–S4 (Supporting Information).

2.2.6. Fluorescence Measurements

Selectivity Studies Using FITC-Tagged Lectins: Resin–Glc (**4**) was tested for selectivity toward lectins: FITC–Con A and FITC–PNA. Briefly, Resin–Glc (**4**) (0.14 mg) was initially treated with 1 mL of bovine serum albumin (BSA; 1 mg mL^{-1} solution) to prevent any nonspecific interactions. These pretreated resins were subsequently exposed to either 0.5 mg mL^{-1} FITC–Con A/FITC–PNA. Upon interaction with FITC-labeled lectins, the resins would retain the fluorescent lectin, to which it is selective for; thereby, the fluorescence intensity of the supernatant solution was reduced, which was measured.

Procedure for Bacterial Sequestration Using SYBR Green I Tagged Cells: The kinetics of bacterial sequestration was monitored using SYBR Green I tagged *E. coli* and *S. aureus* cells aided by fluorescence spectroscopy. SYBR Green I was reported to be the most sensitive fluorescent dye for rapid staining compared to the existing dyes used for fluorescence-based measurements.[68] This method simplifies the quantification of bacterial cells in aqueous media both in terms of sensitivity and time. SYBR Green I stock solution was prepared and stored at −20 °C. Working solutions of the dye were freshly prepared every day prior to the experiment using sterile filtered (0.22 µm, polyvinylidene fluoride (PVDF)) PBS. Unless otherwise stated, the staining experiments were performed using 1 mL of bacterial solution and 20 µL working solution of SYBR Green I, incubated at room temperature in dark. Fluorescence measurements were performed using a Jasco FP 8500 fluorimeter at an excitation/emission wavelength of 485/520 nm. Spectra were obtained with a resolution of 5.0 nm for both excitation and emission at a scan rate of 400 nm min^{-1}, unless otherwise mentioned. All measurements were carried out in a quartz cell of 1 cm path length. All the fluorescence analyses of culture samples were performed in triplicate.

A preliminary bacterial sequestration kinetic study of Resin–Glc (**4**) was performed for a period of 20 h using SYBR Green I tagged *E. coli* cells and the decrease in fluorescence intensity of the solution was found after every hour. This experiment was

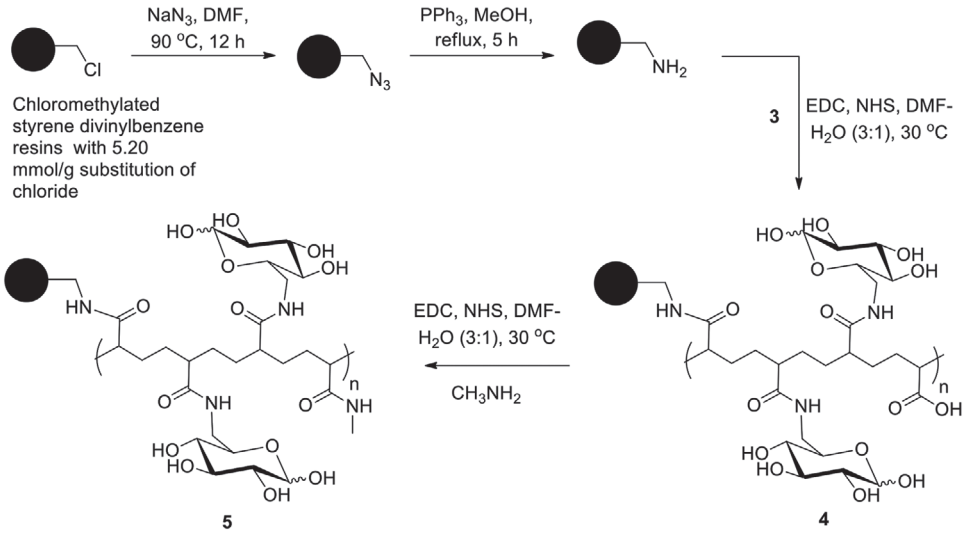

Scheme 2. Synthesis of Glc–AA-functionalized resins.

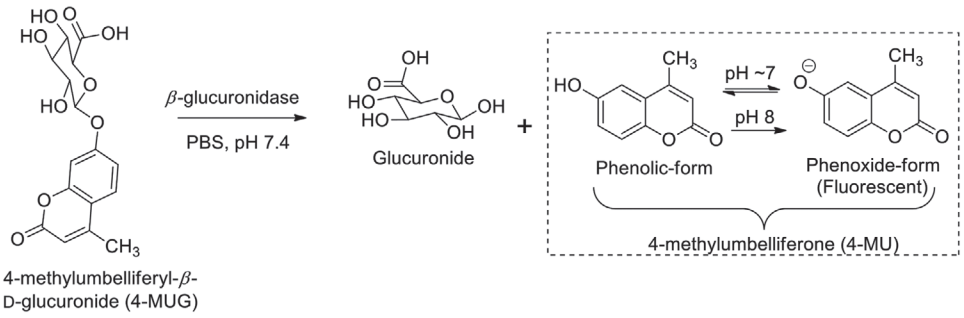

Scheme 3. Enzymatic hydrolysis of 4-methylumbelliferyl-β-D-glucuronide (4-MUG).

carried out by agitating 0.14 g of Resin–Glc (**4**) (pretreated with 1 mg mL^{-1} of BSA solution) with 1 mL of 10^7 CFU mL^{-1} SYBR Green I tagged *E. coli* suspension taken in a centrifuge tube. A known bacterial suspension solution without resin was also agitated under the same conditions for the same period of time.

Procedure for Enzymatic Colorimetric Assay Using 4-MUG: The detection of *E. coli* cells using 4-MUG is based on selective enzymatic hydrolysis of 4-MUG by β-GUS, secreted by >98% of all known *E. coli* strains.

During hydrolysis of 4-MUG using β-GUS, a coumarin derivative, 4-methylumbelliferone (4-MU), which gives emission centered at 440 nm upon excitation at 365 nm, and a glucuronide unit were formed (**Scheme 3**). Subsequent to enzymatic hydrolysis, for a stipulated period of time, the pH of the reaction media was raised to pH 8 using 1 M NaOH for fluorescence measurements.[69]

2.2.7. Sample Preparation for Enzymatic Reactions

The kinetics of the enzymatic reaction of β-GUS and 4-MUG was recorded in sequential measurements by fluorescence spectroscopy at three different β-GUS concentrations 0.05×10^{-6}, 0.10×10^{-6}, and 0.20×10^{-6} M. The enzymatic reaction was carried out in aqueous buffered solution (PBS, pH 7.4) because the optimal pH for the activity of the enzyme is around 7.[69] Briefly, each concentration of β-GUS in PBS buffer (1 mL) was treated with 50 µL of 4-MUG (0.20×10^{-3} M) in a cuvette and immediately fluorescence (an excitation wavelength of 365 nm) was recorded for a period of ≈20 min with an interval of 1 min.

2.2.8. Bacterial Capture and Detection Using Resin–Glc (4) in Syringe Column

A 5 mL syringe column was loaded with 1.00 g of dry Resin–Glc (**4**) and was equilibrated with filtered PBS for 1 h, then drained completely. These resins were pretreated with 2 mL of 2 mg mL^{-1} BSA solution for 30 min to prevent any nonspecific interactions. The *E. coli* cells with a concentration of 10^7 CFU mL^{-1} (1 mL) were added to the syringe column and equilibrated with frequent agitation. The agitation of the resins increases the rate of collision between bacterial cells and ligands on the resin surface.[70] After 3 h, the drained out solution was treated with lysis agent, B-PER reagent (100 µL), to liberate the enzyme β-glucuronidase, followed by 50 µL of 4-MUG (0.2×10^{-3} M) from a freshly prepared stock solution. The solution was incubated at 40 °C for ≈20 min, and the pH of the test solution was raised to pH 8, using 1 M NaOH, before the fluorescence was recorded. The fluorescence observed was subsequently correlated to the number of cells from the 4-MUG calibration plot. To quantify the *E. coli* cells captured on the Resin–Glc (**4**) surface, 100 µL of lysis agent was added to the syringe column and drained after equilibrating for 10 min. The resin was further washed with 3 × 300 µL PBS buffer. The combined solution (1 mL) was subjected to the same procedure mentioned above to quantify the *E. coli* captured by Resin–Glc (**4**).

2.2.9. Bacterial Capture from Artificially Contaminated Tap Water

In order to investigate the sensitivity of the assay, 1 mL of tap water was collected and 1 mL of 1% w/v solution of sodium thiosulfate was added to dechlorinate the water sample prior to the assay. After homogenization of test solution, ≈10^4 CFU *E. coli* cells were added. The mixture was vortexed and divided into two aliquots of 1 mL each. Bacterial concentration in one of the aliquot was measured by fluorescent colorimetric assay using MUG as described previously and the second portion (1 mL) was transferred to Resin–Glc column for bacterial capture studies. Similarly, the tap water samples with different concentrations of *E. coli* ranging from 10^2 to 10^7 CFU mL^{-1} were prepared and analyzed.

3. Results

The change in hydrophilicity of Resin–Cl upon glycopolymer (Glc–AA) functionalization can be visually observed when the resins are immersed in water (**Figure 2**A,B). Resin–Glc (**4**) is more hydrophilic then Resin–Cl which is an important requirement that facilitates the interaction of the former with bacterial cells in the media. The average sizes of the resins were found to be 0.7–1.0 mm in diameter (Figure 2C). The histogram and photograph of Resin–Cl and Resin–Glc in dry condition are given in Figure S5 (Supporting Information).

During each step of functional transformation (Scheme 2), the resins were characterized by FTIR analysis (**Figure 3**). IR spectrum of chloromethylated polystyrene divinylbenzene resins (Resin–Cl) showed characteristic bands at 669 cm^{-1} corresponding to C—Cl stretching. Band at 1264 cm^{-1} was assigned to CH_2 wagging while bands at 1446, 1508, 1604, and 3026 cm^{-1}

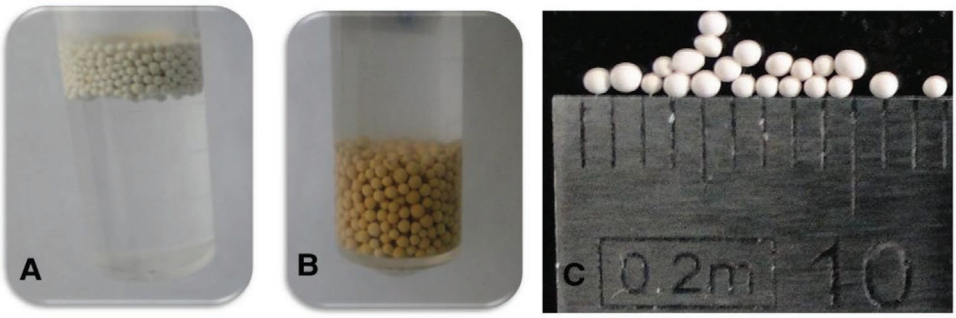

Figure 2. Photographic image of A) Resin–Cl, B) Resin–Glc (**4**), and C) size of the resin (Resin–Cl).

were attributed to C=C (aromatic) and band at 2924 cm^{-1} was due to CH stretching (Figure 3A). During the reaction of Resin–Cl with sodium azide, the band at 669 cm^{-1} vanished with the appearance of a new band at 2090 cm^{-1} indicating the substitution of chloride in Resin–Cl with azide functionality (Figure 3B). In the next step, conversion of azide to amine by Staundinger reduction was monitored by the disappearance of the azide band at 2090 cm^{-1} and with the emergence of a broad band at 3053 cm^{-1}. The presence of the $-CH_2-NH_2$ group is further confirmed by the C—N stretching band at 1197 cm^{-1} as well as N—H bending band at 722 cm^{-1} (Figure 3C). Coupling of Glc–AA to the Resin–NH_2 was validated by the presence of amide band at 1646 cm^{-1}. The presence of glucose units is indicated by the presence of C—H vibrational band at 2915 cm^{-1} and broad O—H vibrational stretching band ranging from 3497 to 3106 cm^{-1}. A combination band of OCH and COH deformations is present at 1512, 1423, and 1121 cm^{-1}. The band at 1082 cm^{-1} corresponds to —C—O—C— stretching frequency, which confirms the presence of pyranose ring (Figure 3D). Bands at 1735 cm^{-1} (—C=O stretching) and 1251 cm^{-1} (—C—O stretching) are attributed to residual carboxylate group present in the glycopolymer attached to resin.

To understand the loading/substitution of amine in the resin, combustion elemental analysis of Resin–Cl and Resin–N_3 was performed using Euro Vector EA 3000 instrument, which gave 6.9% of nitrogen in Resin–N_3. This corresponds to 0.49 mol of nitrogen content in 100 g of resin, i.e., 7.9% of amine in mass. The residual 92.1 g is considered as the resin base material, which contains 0.52 mol of chloride groups on which amine substitution has taken place. The amine substitution ratio was calculated as (0.49/0.52) 94% with respect to chlorine. The glycopolymer content on the Resin–Glc was determined to be

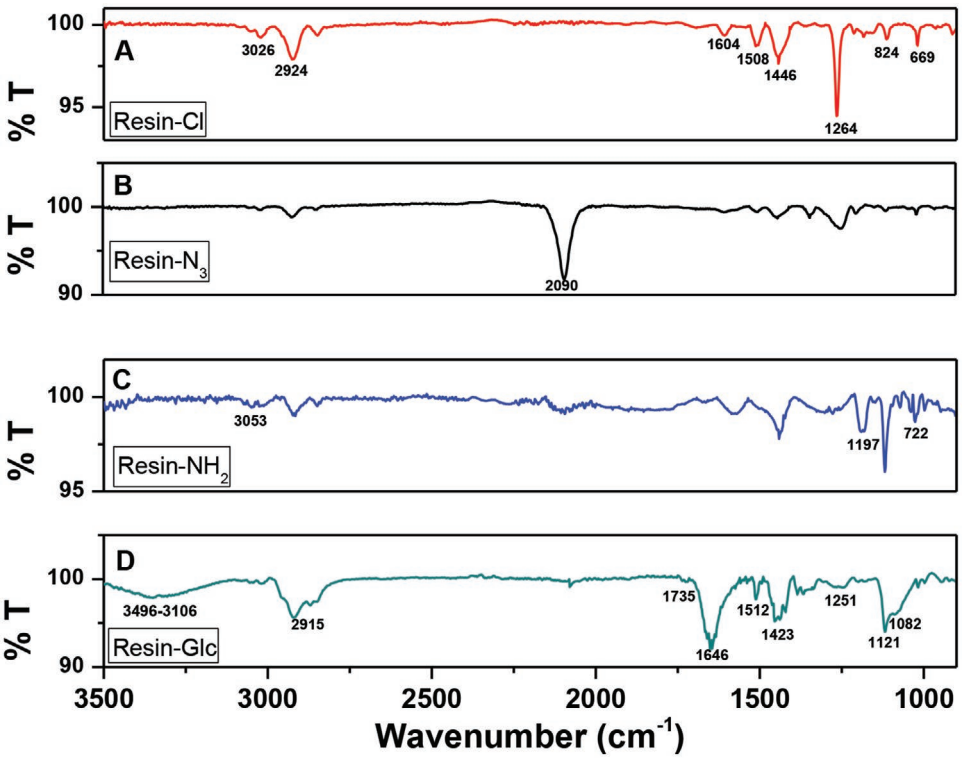

Figure 3. FTIR spectra of A) Resin–Cl, B) Resin–N_3, C) Resin–NH_2, and D) Resin–Glc (**4**).

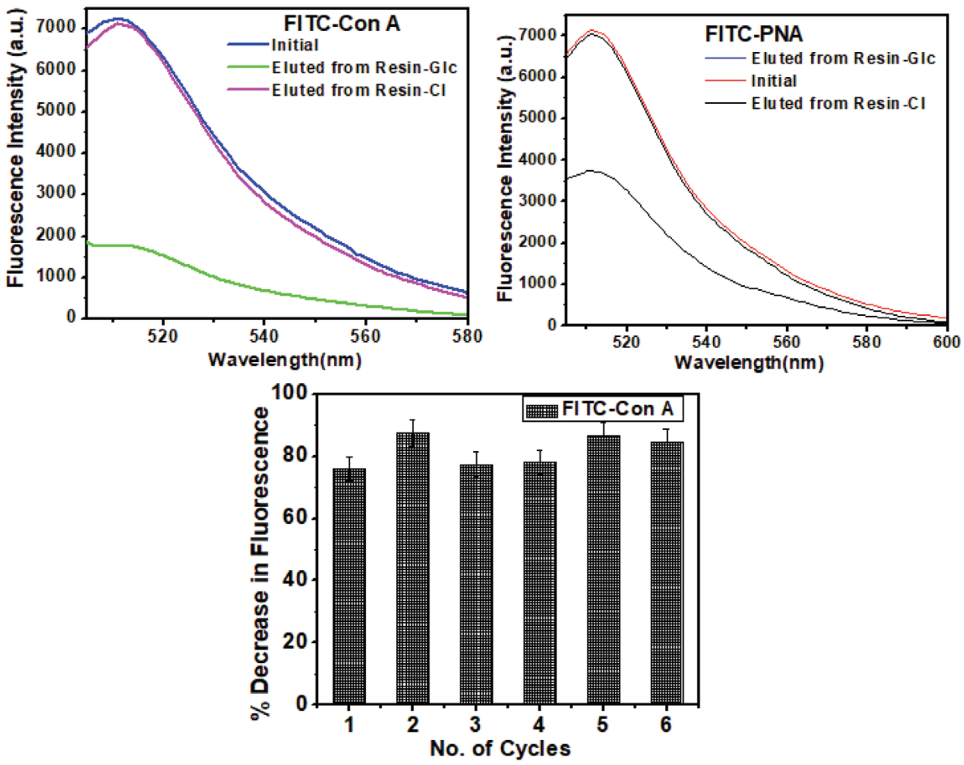

Figure 4. Decrease in fluorescence intensity of A) FITC–Con A, B) FITC–PNA, C) percentage decrease in fluorescence intensity of FITC–Con A over six cycles upon interaction with Resin–Glc (**4**).

5 wt% of the resin base material using thermogravimetric analysis (Figure S6, Supporting Information).

3.1. Specific Lectin Recognition and Reusability Studies on Resin–Glc (4)

The binding potential and selectivity of the prepared Resin–Glc (**4**) for lectin were studied using Con A and PNA, which are specific lectins for binding glucose/mannose and galactose residues, respectively. Additionally, BSA with a molecular weight comparable to Con A, but without glucose-binding domains, was chosen as a "nonspecific protein." With these model systems, the interaction behavior between the lectin and glucose units present on the surface of the resin was studied. For studying the interaction using fluorescence spectroscopy, FITC-labeled Con A and PNA were employed. **Figure 4**A,B shows the fluorescence emission spectra of FITC-labeled Con A and PNA solutions before and after interaction with Resin–Glc (**4**). A significant reduction in the emission intensity up to 81.7 ± 5% was observed in FITC–Con A solution upon interaction with Resin–Glc (**4**) whereas only 47 ± 5% reduction was observed for FITC–PNA. However, no significant reduction in fluorescence intensity was observed when the Resin–Cl was treated with the lectin solutions. The effect of nonspecific interactions in Resin–Glc was studied using FITC–BSA under similar conditions, which exhibited no significant reduction in emission intensity (Figure S7, Supporting Information).

After each cycle, Resin–Glc (**4**) was washed with excess of mannose/galactose to recover the resins from Con–A/PNA bound to it. Subsequently, resins were rinsed with PBS solution. The recovered resins were then subjected to six cycles of experiments. Figure 4C shows the percentage decrease in fluorescence intensity over each cycle. From the bar diagram it is clear that percentage decrease in fluorescence intensity remained consistent over six cycles of experiments, and hence demonstrates the capture efficiency and reusability of Resin–Glc (**4**) for Con A detection.

3.2. Bacterial Sequestration Kinetics Using Resin–Glc (4)

Consequent to the satisfying findings using Con A, the studies were extrapolated to *E. coli*, which contain fimH protein, a lectin that is present on type 1 fimbria of *E. coli*, which can specifically recognize glucose/mannose containing ligands by carbohydrate–lectin interaction.[71,72] Fluorescence measurements using SYBR Green I tagged *E. coli* cells, at an excitation wavelength of 485 nm, revealed that about 45% decrease in the fluorescence intensity of SYBR Green I was achieved within 5 h of interaction of *E. coli* with Resin–Glc (**4**). On the contrary, only 4% decrease in fluorescence intensity was observed in the case of *S. aureus*, which further remained unaltered throughout the experimental period (**Figure 5**). However, no substantial change in the fluorescence intensity was observed in the absence of the resin.

The relevance of calcium ions in the buffer solution used for bacterial capture has been reported in many studies.[73,74] In order to check the same in Resin–Glc (**4**), bacterial sequestration was conducted in the presence and absence of calcium. In

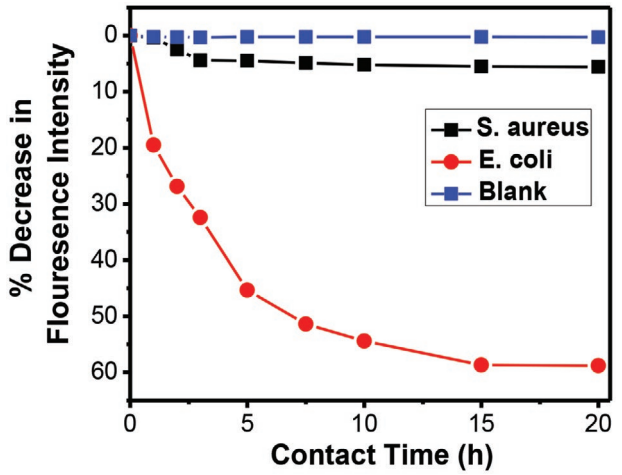

Figure 5. Kinetics of bacterial sequestration using SYBR Green I tagged *E. coli* and *S. aureus* cells in contact with Resin–Glc (**4**).

the absence of calcium, consistent results were not observed during multiple cycles of experiments using Resin–Glc (**4**). This could be because of the free carboxylate groups present in Resin–Glc (**4**), whose negative charges could repel the negatively charged cell membrane of the bacterial cells. In order to confirm this hypothesis, we converted the residual carboxylic acid groups present in Resin–Glc (**4**) to amide functionalities by coupling with methyl amine using EDC–NHS as shown in Scheme 2. The resultant amide-modified Resin–Glc–$MeNH_2$ (**5**) was subjected to bacterial sequestration cycles as mentioned for Resin–Glc (**4**). Satisfyingly, the experiments with Resin–Glc–$MeNH_2$ (**5**) in buffer with/without Ca^{2+} ions yielded results very similar to that obtained with Resin–Glc (**4**) in buffer containing excess Ca^{2+} ions. This observation suggests that the Ca^{2+} ions present in the buffer might help to crosslink the residual carboxylate groups present in Resin–Glc (**4**) to furnish consistent results. These results corroborate the importance of masking negatively charged species in the studies involving *E. coli* detection. Hence, in further studies using Resin–Glc (**4**), buffer containing Ca^{2+} ions was used as an appropriate medium.

3.3. Kinetics of the Enzymatic Reaction of β-GUS with 4-MUG

The kinetic study of the reaction of 4-MUG with varying concentrations of β-GUS (0.05×10^{-6}, 0.10×10^{-6}, and 0.20×10^{-6} M) showed a monotonous increase in fluorescence emission intensity with reaction time at the emission wavelength (λ_{max} = 440 nm) in aqueous buffered solution. The emission reached saturation in ≈20 min for 0.10×10^{-6} and 0.20×10^{-6} M β-GUS under the conditions employed (Figure S8B,C, Supporting Information). At 0.05×10^{-6} M the reaction proceeded very slowly and did not reach completion even after 20 min (Figure S8A, Supporting Information). On the contrary, in the enzyme-free buffer, no emission due to 4-MU was detected. The initial apparent reaction rate was found to increase linearly with initial enzyme concentration, which is in agreement with the Michaelis–Menten kinetics (Figure S8D, Supporting Information).[75] The limit of detection (LOD) of β-GUS was calculated based on the above results as shown in Figure S9 (Supporting Information).

3.4. Calibration Plot of 4-MUG and LOD of *E. coli* Cells

The emission of the released deprotonated 4-MU can be easily detected when observed under conventional UV illumination (Figure S10, inset, Supporting Information). The photographic image under UV illumination clearly distinguishes the *E. coli* cell concentration based on the emission from 4-MU.

A good fit calibration plot for *E. coli* cells using 4-MUG (0.20×10^{-3} M) in aqueous buffered solution was acquired with correlation coefficient $R^2 = 0.98$ as shown in Figure S10 (Supporting Information). The working linear range was between 10^2 and 10^6 CFU mL^{-1} by fitting to linear least square relationship. Commonly LOD is calculated as nonspecific signal or blank plus three times standard deviation of the nonspecific signal. Since the blank signal was negligible, the calculated LOD was found to be very low,[76] which is an unrealistic value to report and is not usually used. The lowest limit of detection was thus set as the lowest concentration in the linear range, which is 10^3 CFU mL^{-1}.

3.5. Syringe Column-Based Capture and Detection of *E. coli* Using Resin–Glc (4)

The results in Section 3.2, using SYBR Green I dye, encouraged us to use Resin–Glc (**4**) in the form of a reusable solid support filled in a syringe column which can be utilized for *E. coli* capture and detection. As a preliminary study, 1 mL of *E. coli* cell suspension of a concentration of 10^7 CFU mL^{-1} was equilibrated in a syringe column loaded with 1.00 g of Resin–Glc (**4**), as shown in **Figure 6**A. The number of cells captured by Resin–Glc (**4**) and the residual cells drained out of the column were determined (Figure 6B) as per Section 2.2.8. The fluorescence data upon correlation with the 4-MUG calibration plot revealed that 10^5 cells were captured in the column and the residual solution contained ≈10^2 cells (Figure 6C).

3.6. Reusability and Capture Efficiency of Resin–Glc (4) in Column

The reusability and capture efficiency of the bacterial capture matrix are important parameters to be explored in order to understand how economically benign is the system. For reusability of the matrix, efficient release of the captured bacteria is vital. There are many approaches which have been reported to release the attached bacteria from the surfaces using various external stimuli.[77–83] Having explored the reversible binding and release of Con A using mannose as the external stimuli, the resin surface is also anticipated to release the captured bacteria using the same mannose solution. In this experimental protocol, every capture event was followed by cell lysis to quantify the *E. coli* cells captured by Resin–Glc (**4**); subsequently, the resins were washed with high concentration of mannose (300×10^{-3} M) for 0.5 h and then with PBS buffer to regenerate

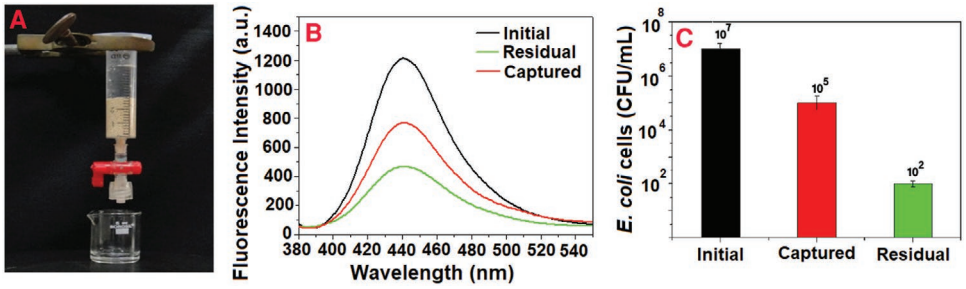

Figure 6. A) Photographic image of the syringe column loaded with Resin–Glc (**4**). B) Fluorescence spectra corresponding to *E. coli* cells upon enzymatic reaction with MUG: initial cells added to the column (black); cells captured in the column (red); and cells drained out of the column (green). C) Quantification of *E. coli* cells upon correlation of fluorescence intensity with 4-MUG calibration plot.

the resin for the next cycle. The capture efficiency of Resin–Glc (**4**) was studied by varying the initial concentration of *E. coli* cells from 10^5 to 10^8 CFU mL^{-1}. In every cycle, the *E. coli* cells were given an interaction time of 3 h with the resin. It was observed that the capture efficiency of the resin depends on contact time vide supra (Figure 5) and also on the amount of resin loaded in the column. Therefore, in the present study using 1.00 g of Resin–Glc (**4**), keeping contact time 3 h, at different initial *E. coli* concentrations, the maximum bacterial load of Resin–Glc (**4**) was found to be 10^5 cells g^{-1} of resin (**Figure 7**). This result was consistent up to 10^7 CFU mL^{-1} of initial *E. coli* concentration whereas for higher initial concentrations lower capture efficiency was observed reflecting gradual saturation of the resin surface.[84]

Based on the above results, in order to understand the reusability of Resin–Glc (**4**), the capture-and-release cycles were repeated with an initial *E. coli* cell concentration of 10^7 CFU mL^{-1} for six cycles (keeping the interaction period 3 h). It was observed that the resin surface was efficiently regenerated using the protocol mentioned (Section 2.2.8) vide supra after every cycle, without any decrease in capture efficiency as is evident from **Figure 8**. The capture efficiency was ≈10^5 CFU g^{-1} of Resin–Glc (**4**) in all the six cycles. The high capability for capture as well as ease of detection of specific bacteria and the regeneration of the capture matrix are of the utmost importance for many practical applications such as continuous detection of bacteria and downstream bacterial diagnostics.[55]

3.7. Detection of *E. coli* in Tap Water

The performance of Resin–Glc-based column for detection of *E. coli* in real samples was evaluated using tap water spiked with different cell densities of *E. coli* (10^2–10^7 CFU mL^{-1}). The results obtained (**Figure 9**) after equilibration (3 h) of contaminated tap water with 1.00 g of Resin–Glc, filled in a column, were found to be satisfactory. It can be observed that beyond 10^5 CFU mL^{-1}, the capture efficiency decreases significantly; this observation is in agreement with the capture capacity (≈10^5 CFU g^{-1}) of 1.00 g resin-filled column. Thus, the method portrayed is useful for the detection of *E. coli* in real samples with cell densities (10^2–10^5 CFU mL^{-1}). The fluorescence intensity was obtained by using 4-MUG as the enzymatic substrate for each of the cell densities based on the procedure mentioned before.

4. Conclusion

In summary, we have developed an economically benign and reusable resin-based solid support for efficient capture and

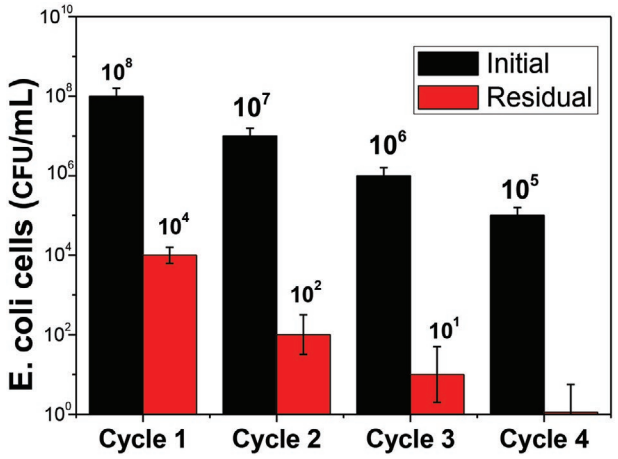

Figure 7. Bar diagram depicting the capture efficiency of Resin–Glc (**4**) over four cycles at varying *E. coli* concentrations.

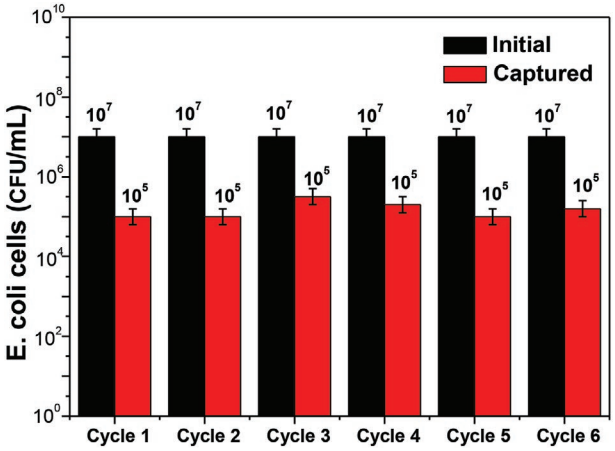

Figure 8. Bar diagram depicting the reusability of Resin–Glc (**4**) over six cycles.

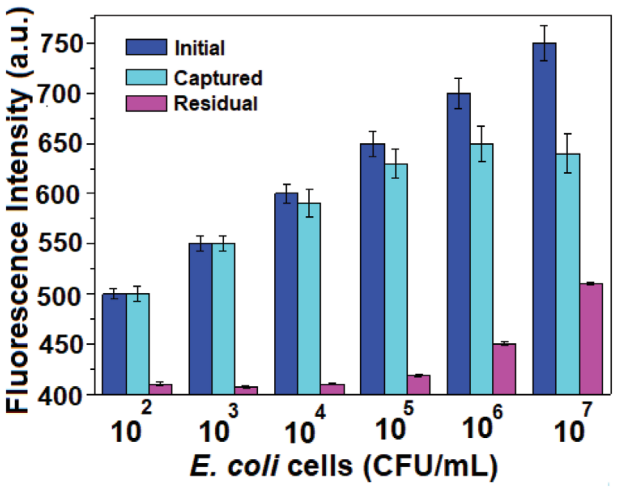

Figure 9. Quantification of *E. coli* cells spiked in tap water sample using the Resin–Glc column.

release of *E. coli*. This resin-based platform was developed by functionalizing a commercially available chloromethylated styrene divinyl benzene resin with D-glucose based glycopolymer (Glc–AA) in few synthetic steps. The "glycocluster effect" presented by the glucose units on the resin surface is utilized to specifically bind glucose/mannose-binding proteins like Con A and fimH positive bacteria (type 1 fimbriated *E. coli*). Due to the noncovalent nature of interaction, the resin surface can be easily regenerated after cell lysis and subsequent washings using mannose solution. The *E. coli* cells captured by Resin–Glc (**4**) can be quantified by *β*-glucuronidase-based enzymatic assay using 4-MUG. The LOD value for *E. coli* cells determined by using the 4-MUG calibration plot was found to be 10^3 CFU mL^{-1}. The quick (≈20 min) and easy enzymatic reaction with 4-MUG facilitated to quantify the capture efficiency of Resin–Glc (**4**), which was found to be 10^5 CFU g^{-1} of resin over 3 h of *E. coli* cell incubation. The capture efficiency of the resin remained consistent for up to six experimental cycles. The robust method of synthesis of Resin–Glc (**4**) and efficient colorimetric detection make the current system a promising platform for large scale applications.

Supporting Information

Supporting Information is available from the Wiley Online Library or from the author.

Acknowledgements

The authors are thankful to Dr. Sunil K. Ghosh, Associate Director, Bio-Science Group & Head, BOD, and Dr. Awadhesh Kumar, Head, RPCD for their constant support and encouragement.

Conflict of Interest

The authors declare no conflict of interest.

Keywords

capture, detection, *Escherichia coli*, glycoacrylamide, glycopolymer, resin

Received: September 25, 2020
Revised: November 27, 2020
Published online:

[1] R. G. V. Merwe, P. D. van-Helden, R. M. Warren, S. L. Sampson, N. C. Gey van Pittius, *Analyst* **2014**, *139*, 2617.
[2] Y. Jiang, S. Zou, X. Cao, *Anal. Methods* **2016**, *8*, 6668.
[3] H. S. Xu, N. Roberts, F. L. Singleton, R. W. Attwell, D. J. Grimes, R. R. Colwell, *Microb. Ecol.* **1982**, *8*, 313.
[4] T. Ramamurthy, A. Ghosh, G. P. Pazhani, S. Shinoda, *Front. Public Health* **2014**, *2*, 103.
[5] B. S. Ferguson, S. F. Buchsbaum, T.-T. Wu, K. Hsieh, Y. Xiao, R. Sun, H. T. Soh, *J. Am. Chem. Soc.* **2011**, *133*, 9129.
[6] J. L. Bono, J. E. Keen, L. C. Miller, J. M. Fox, C. G. Chitko-McKown, M. P. Heaton, W. W. Laegreid, *Appl. Environ. Microbiol.* **2004**, *70*, 1855.
[7] E. C. Alocilja, S. M. Radke, *Biosens. Bioelectron.* **2003**, *18*, 841.
[8] P. Elizaquível, G. Sánchez, R. Aznar, *Food Control* **2012**, *25*, 704.
[9] N. Jothikumar, M. W. Griffiths, *Appl. Environ. Microbiol.* **2002**, *68*, 3169.
[10] W. Ju, A.-L. Moyne, M. L. Marco, *Front Microbiol.* **2016**, *7*, 223.
[11] A. Roda, M. Mirasoli, B. Roda, F. Bonvicini, C. Colliva, *Microchim. Acta* **2012**, *178*, 7.
[12] P. Belgrader, W. Benett, D. Hadley, G. Long, R. Mariella, F. Milanovich Jr., S. Nasarabadi, W. Nelson, J. Richards, P. Stratton, *Clin. Chem.* **1998**, *44*, 2191.
[13] P. Belgrader, C. J. Elkin, S. B. Brown, S. N. Nasarabadi, R. G. Langlois, F. P. Milanovich, B. W. Colston, G. D. Marshall, *Anal. Chem.* **2003**, *75*, 3446.
[14] V. Chizhikov, A. Rasooly, K. Chumakov, D. D. Levy, *Appl. Environ. Microbiol.* **2001**, *67*, 3258.
[15] J. R. Stults, O. Snoeyenbos-West, B. Methe, D. R. Lovley, D. P. Chandler, *Appl. Environ. Microbiol.* **2001**, *67*, 2781.
[16] L. Westin, C. Miller, D. Vollmer, D. Canter, R. Radtkey, M. Nerenberg, J. P. O'Connell, *J. Clin. Microbiol.* **2001**, *39*, 1097.
[17] A. T. Woolley, K. Lao, A. N. Glazer, R. A. Mathies, *Anal. Chem.* **1998**, *70*, 684.
[18] M. Barreiros dos Santos, J. P. Agusil, B. Prieto-Simón, C. Sporer, V. Teixeira, J. Samitier, *Biosens. Bioelectron.* **2013**, *45*, 174.
[19] H. Bridle, B. Miller, M. P. Y. Desmulliez, *Water Res.* **2014**, *55*, 256.
[20] R. T. Noble, S. B. Weisberg, *J. Water Health* **2005**, *3*, 381.
[21] X. Liu, S. Wang, *Chem. Soc. Rev.* **2014**, *43*, 2385.
[22] M. Lin, J. F. Chen, Y. T. Lu, Y. Zhang, J. Song, S. Hou, Z. Ke, H. R. Tseng, *Acc. Chem. Res.* **2014**, *47*, 2941.
[23] Z. Qi, P. Bharate, C. H. Lai, B. Ziem, C. Bottcher, A. Schulz, F. Beckert, B. Hatting, R. Mulhaupt, P. H. Seeberger, R. Haag, *Nano Lett.* **2015**, *15*, 6051.
[24] W. Zhan, Y. Qu, T. Wei, C. Hu, Y. Pan, Q. Yu, H. Chen, *ACS Appl. Mater. Interfaces* **2018**, *13*, 10647.
[25] C. Hu, J. Wu, T. Wei, W. Zhan, Y. Qu, Y. Pan, Q. Yu, H. Chen, *J. Mater. Chem. B* **2018**, *6*, 2198.
[26] K. Stevens, L. Jaykus, *Crit. Rev. Microbiol.* **2004**, *30*, 7.
[27] M. Uyttendaele, I. Van Hoorde, J. Debevere, *Int. J. Food Microbiol.* **2000**, *54*, 205.
[28] A. G. Gehring, P. L. Irwin, S. A. Reed, S.-I. Tu, P. E. Andreotti, H. Akhavan-Tafti, R. S. Handley, *J. Immunol. Methods* **2004**, *293*, 97.
[29] S. P. Ravindranath, L. J. Mauer, C. Deb-Roy, J. Irudayaraj, *Anal. Chem.* **2009**, *81*, 2840.

[30] Y. Zhao, M. Ye, Q. Chao, N. Jia, Y. Ge, H. Shen, *J. Agric. Food Chem.* **2009**, *57*, 517.
[31] Y. Wang, P. Fewins, E. C. Alocilja, *IEEE Sens. J.* **2015**, *15*, 4692.
[32] R. Joshi, H. Janagama, H. P. Dwivedi, T. M. A. Senthil Kumar, L. Jaykus, J. Schefers, S. Sreevatsan, *Mol. Cell. Probes* **2009**, *23*, 20.
[33] S. Wu, N. Duan, Z. Shi, C. Fang, Z. Wang, *Anal. Chem.* **2014**, *86*, 3100.
[34] S. Poshtiban, M. A. Javed, D. Arutyunov, A. Singh, G. Banting, C. M. Szymanski, S. Evoy, *Analyst* **2013**, *138*, 5619.
[35] K. El-Boubbou, C. Gruden, X. Huang, *J. Am. Chem. Soc.* **2007**, *129*, 13392.
[36] Y. Wang, S. Ravindranath, J. Irudayaraj, *Anal. Bioanal. Chem.* **2011**, *399*, 1271.
[37] D. Hor'ak, M. Babic, H. Mackov'a, M. J. Benes, *J. Sep. Sci.* **2007**, *30*, 1751.
[38] H. K. Lau, L. M. Clotilde, A. P. Lin, G. L. Hartman, C. R. Lauzon, *J. Lab. Autom.* **2013**, *18*, 178.
[39] J. Chen, X. Shi, A. G. Gehring, G. C. Paoli, *Int. J. Food Microbiol.* **2014**, *179*, 33.
[40] Y. Wang, J. K. Salazar, *Compr. Rev. Food Sci. Food Saf.* **2016**, *15*, 183.
[41] A. D. Taylor, J. Ladd, Q. Yu, S. Chen, J. Homola, S. Jiang, *Biosens. Bioelectron.* **2006**, *22*, 752.
[42] J. Waswa, J. Irudayaraj, C. DebRoy, *LWT-Food Sci. Technol.* **2007**, *40*, 187.
[43] S. Chen, V. C. H. Wu, Y. Chuang, C. Lin, *J. Microbiol. Methods* **2008**, *73*, 7.
[44] Y. Wang, R. Wang, Y. Li, B. Srinivasan, S. Tung, H. Wang, M. F. Slavik, C. L. Griffis, *Biol. Eng.* **2010**, *2*, 49.
[45] G. Pasparakis, C. Alexander, *Analyst* **2007**, *132*, 1075.
[46] V. N. Tra, D. H. Dube, *Chem. Commun.* **2014**, *50*, 4659.
[47] E. K. Wujcik, H. Wei, X. Zhang, J. Guo, X. Yan, N. Sutrave, S. Wei, Z. Guo, *RSC Adv.* **2014**, *4*, 43725.
[48] N. Duan, S. Wu, S. Dai, H. Gu, L. Hao, H. Ye, Z. Wang, *Analyst* **2016**, *141*, 3942.
[49] A. K. Adak, H.-J. Lin, C.-C. Lin, *Org. Biomol. Chem.* **2014**, *12*, 5563.
[50] S.-K. Wang, C.-M. Cheng, *Chem. Commun.* **2015**, *51*, 16750.
[51] C. Müller, G. Despras, T. K. Lindhorst, *Chem. Soc. Rev.* **2016**, *45*, 3275.
[52] M. Varshney, Y. Li, *Biosens. Bioelectron.* **2009**, *24*, 2951.
[53] A. Kausaite-Minkstimiene, A. Ramanaviciene, J. Kirlyte, A. Ramanavicius, *Anal. Chem.* **2010**, *82*, 6401.
[54] J. A. Goode, J. V. H. Rushworth, P. A. Millner, *Langmuir* **2015**, *31*, 6267.
[55] B. Rotman, *Bacteriol. Rev.* **1960**, *24*, 251.
[56] A. D. Treweek, J. J. Morgan, *J. Colloid Interface Sci.* **1977**, *60*, 258.
[57] L. T. Lui, X. Xue, C. Sui, A. Brown, D. I. Pritchard, N. Halliday, K. Winzer, S. M. Howdle, F. Fernandez-Trillo, N. Krasnogor, C. Alexander, *Nat. Chem.* **2013**, *5*, 1058.
[58] N. Kawabata, T. Inoue, H. Tomita, *Epidemiol. Infect.* **1992**, *108*, 123.
[59] S. R. S. Ting, E. H. Min, P. B. Zetterlund, M. H. Stenzel, *Macromolecules* **2010**,*43*, 5211.
[60] A. Muñoz-Bonilla, M. Fernández-García, *Materials* **2015**, *8*, 2276.
[61] M. Álvarez-Paino, V. Bordegé, R. Cuervo-Rodríguez, A. Muñoz-Bonilla, M. Fernández-García, *Macromol. Chem. Phys.* **2014**, *215*, 1915.
[62] G. Chen, G. Mantovani, L. Tao, J. Geng, D. Nystro, D. M. Haddleton, *Macromolecules* **2007**, *40*, 7513.
[63] A. Pfaff, L. Barner, A. H. E. Müller, A. M. Granville, *Eur. Polym. J.* **2011**, *47*, 805.
[64] M. Álvarez-Paino, A. Muñoz-Bonilla, G. Marcelo, J. Rodríguez-Hernández, M. Fernández-García, *Polym. Chem.* **2012**, *3*, 3282.
[65] J. K. Ajish, A. B. Kanagare, K. S. A. Kumar, M. Subramanian, A. D. Ballal, M. Kumar, *ACS Appl. Nano Mater.* **2020**, *3*, 1307.
[66] J. K. Ajish, K. S. A. Kumar, M. Subramanian, M. Kumar, *Sens. Actuators, B* **2018**, *255*, 1726.
[67] J. K. Ajish, K. S. A. Kumar, M. Subramanian, M. Kumar, *RSC Adv.* **2014**, *4*, 59370.
[68] W. Martens-Habbena, H. Sass, *Appl. Environ. Microbiol.* **2006**, *72*, 87.
[69] C. Briciu-Burghina, B. Heery, F. Regan, *Analyst* **2015**, *140*, 5953.
[70] S.-I. Tu, J. Uknalis, M. Gore', P. Irwin, I. Feder, *J. Rapid Methods Autom. Microbiol.* **2011**, *11*, 35.
[71] Z. Zhu, J. Wang, A. I. Lopez, F. Yu, Y. Huang, A. Kumar, S. Li, L. Zhang, C. Cai, *Biomater. Sci.* **2015**, *3*, 842.
[72] Y. Qu, T. Wei, W. Zhan, C. Hu, L. Cao, Q. Yu, H. Chen, *J. Mater. Chem. B* **2017**, *5*, 444.
[73] T. Hosoi, Y. Imai, T. Irimura, *Glycobiology* **1998**, *8*, 791.
[74] T. D. R. Vance, S. Guo, S. Assaie-Ardakany, B. Conroy, P. L. Davies, *PLoS One* **2019**, *14*, e0220045.
[75] M.-M. S. Ebrahimi, Y. Voss, H. Schönherr, *ACS Appl. Mater. Interfaces* **2015**, *7*, 20190.
[76] F. C. Dudak, İ. H. Boyac, A. Jurkevica, M. Hossain, Z. Aquilar, H. B. Halsall, C. J. Seliskar, W. R. Heineman, *Anal. Bioanal. Chem.* **2009**, *393*, 949.
[77] Q. Yu, J. Cho, P. Shivapooja, L. K. Ista, G. P. Lopez, *ACS Appl. Mater. Interfaces* **2013**, *5*, 9295.
[78] Q. Yu, L. K. Ista, G. P. Lopez, *Nanoscale* **2014**, *6*, 4750.
[79] P. Shivapooja, Q. Yu, B. Orihuela, R. Mays, D. Rittschof, J. Genzer, G. P. Lopez, *ACS Appl. Mater. Interfaces* **2015**, *7*, 25586.
[80] S. Sankaran, J. Van Weerd, J. Voskuhl, M. Karperien, P. Jonkheijm, *Small* **2015**, *11*, 6187.
[81] T. Wei, Q. Yu, W. Zhan, H. Chen, *Adv. Healthcare Mater.* **2016**, *5*, 449.
[82] B. Xue, M. Qin, J. Wu, D. Luo, Q. Jiang, Y. Li, Y. Cao, W. Wang, *ACS Appl. Mater. Interfaces* **2016**, *8*, 15120.
[83] T. Wei, Z. Tang, Q. Yu, H. Chen, *ACS Appl. Mater. Interfaces* **2017**, *9*, 37511.
[84] S. Rotem, N. Raz, Y. Kashi, A. Mor, *Appl. Environ. Microbiol.* **2010**, *76*, 3301.